Universal force correlations in an RNA-DNA unzipping experiment

Kay Joerg Wiese, Mathilde Bercy, Lena Melkonyan, Thierry Bizebard

Universal Force Correlations in an RNA-DNA Unzipping Experiment

Kay Jörg Wiese[1], Mathilde Bercy[2], Lena Melkonyan[2], Thierry Bizebard[3]
[1]*Laboratoire de Physique de l'École Normale Supérieure, ENS, Université PSL, CNRS, Sorbonne Université, Université Paris-Diderot, Sorbonne Paris Cité, 24 rue Lhomond, 75005 Paris, France.*
[2]*UMR 7615, Ecole Supérieure de Physique et Chimie Industrielles de la Ville de Paris, Paris, France.*
[3]*UMR 8104, Institut Cochin, 22 rue Méchain, 75014 Paris, France.*

We study unzipping of a complementary RNA-DNA helix applied to an external force. The force-force correlations are measured, and compared to predictions from an exact solution of a 1-d toy model, as well as field theory based on functional renormalization. Within error bars, the agreement is excellent.

I. INTRODUCTION

The amount of biological data is growing steadily, reaching about 2.5×10^{16} Bytes in 2015 [1], roughly on equal footage with other domains as astronomy, youtube and Twitter. An important question is what can be learned from these data, and what cannot? Depending on their specialisation, scientists usually ask different, and seemingly unrelated questions. Here we study peeling of a complementary RNA-DNA double strand, using a sequence obtained from ribosomal RNA. As shown on Fig. 1, at one end the double helix is attached with its both strands to a bead, whereas on the other end only the DNA-strand is. Pulling on the beads with an optical tweezer [2] the RNA strand peels off. What is measured is the force-extension curve, of which an example is given on Fig. 2.

Rather complementary questions can now be asked:

(i) What can one learn about the specific *biological system*?

(ii) Are there observables which are independent of the chosen nucleotide sequence, thus *universal*?

(iii) How does understanding the *universal signal* help to analyse the *biological system*? What limitations does it impose?

The first question is at the origin and design of the experiment [3–5]. We choose the RNA-sequence from the large subunit of the ribosome.

Consider the force-extension curve on Fig. 2. Applying no force, the RNA-DNA double strand is in an equilibrated coiled state, with its end-to-end distance being roughly $0.8\mu m$. Since the beads are sitting in an optical trap, their distance, or more specifically the distance w between the two minima of the trap, is the control parameter. Increasing w, the RNA-DNA double strand gets stretched, which is reflected in an increase in the measured force F. Finally part of the RNA sequence peels off [7], leading to a first drop in the force-extension curve. Increasing w further leads to more force drops resulting in an *almost* constant force. This *plateau regime* is marked in red on Fig. 2. Increasing w further, peeling can no longer reduce the force, and the latter increases again, eventually leading to the breakage of the DNA molecule (not shown here). If instead of w the applied force F were controled, as in experiments with magnetic tweezers [8, 9], a phase transition at F_c could be observed between a closed and open state [10].

The aim of this letter is to analyse the force fluctuations on the plateau, i.e. the saw-tooth shaped signal on top of the critical force. This kind of signal is frequent in nature, and at the heart of the so-called *depinning transition*: It arises in a plethora of situations: Barkhausen noise in magnets [11, 12]

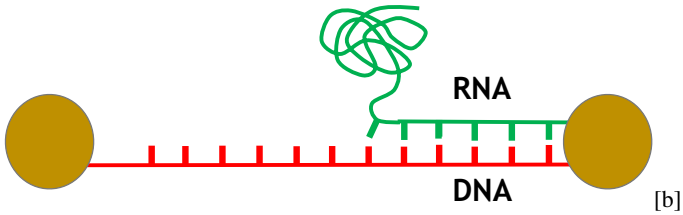

[b]

FIG. 1: Peeling of a RNA-DNA double strand. The RNA sequence is from subunit 23S of the ribosome in E. Coli, prolonged to attach the beads (with a much larger radius than drawn here). The DNA sequence is its complement. The beads are drawn about 10 times smaller than in the experiment.

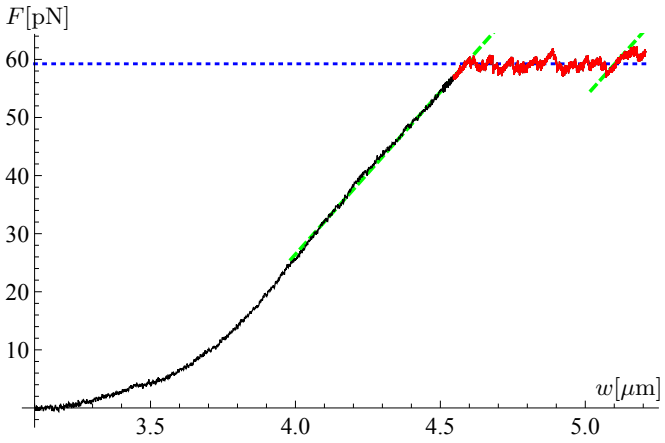

FIG. 2: A sample force-extension curve. For the data-analysis we only use the last part of the curve, the plateau (in red). On this plateau, the force fluctuates around its critical value of about 60pN. The extension w starts at 3μm, which is the sum of the unstretched molecule plus twice the radius of the beads ($2 \times 1\mu m$). The effective stiffness m^2 in Eq. (1) is estimated from the slope of the green dashed lines as $m^2 = 55 \pm 5\mathrm{pN}/\mu\mathrm{m}$ at the beginning of the plateau, which remains at least approximately correct at the end of the plateau. The driving velocity is about $7\mathrm{nm/s}$, corresponding to 42 nucleotides/s as in the cell [6].

(audible as the rustle in old-style telephones), depinning of a contactline [13] (the line where coffee and air meet in a cup, or drops on a windshield), earthquakes [14], vortices in high-temperature superconductors [15], to name a few. The largest such system on earth is the movement of tectonic plates in the outer crust of the earth, where the resulting force drops are earthquakes. The smallest system the authors are aware of is the unzipping experiment studied here. Yet, all these systems have a very similar phenomenology: In each case, a control parameter w is increased, leading to an increase in tension of the elastic object, released via a succession of force drops. Being omnipresent, many theoretical models and mechanisms have been proposed for this *depinning transition*, starting from the chaos induced in the Burridge-Knopoff model of 1967 [16], over toy models for magnets [17, 18], to sophisticated field theoretic work using functional RG [19–24]. Today it is understood that the minimal ingredients are

(i) a random force (the *disorder*),

(ii) an elastic coupling to an external control parameter,

(iii) an overdamped dynamics.

In the experiment considered here, the random force comes from the *seemingly* random RNA sequence of the ribosome [37]. The elastic coupling to an external control parameter is given by the bead attached to the ends of the strands sitting in the harmonic trap at a given distance w. Finally, an overdamped dynamics is typical for small systems immersed into a solvent, where inertia plays a negligible role.

II. THEORY

The measured force can be expressed as [38]

$$F = m^2(w-u)\,, \tag{1}$$

where w is the distance of the second trap from the first one, and u the position of the second bead, s.t. $w-u=0$ if the beads are sitting in the minima of the traps. This corresponds to an energy $\mathcal{E} = \frac{m^2}{2}(w-u)^2$ where m^2 is the strength of the trap and the elasticity of the partially unzipped double strand, taken in series. What is measured in the experiment is the force given in Eq. (1). More interesting to us than its mean $\langle F\rangle \equiv F_{\rm c} \approx 60$pN are its correlations, i.e. the connected expectations

$$\begin{aligned}\Delta(w,w') &:= \langle F(w)F(w')\rangle^{\rm c} \\ &\equiv \big\langle \big[F(w)-\langle F(w)\rangle\big]\big[F(w')-\langle F(w')\rangle\big]\big\rangle\,.\end{aligned} \tag{2}$$

Here w and w' are two distinct positions of the trap (two different values of w in Fig. 2). Two remarks are in order: First, $\langle F(w)\rangle$ should not depend on w, and equal the plateau value shown on Fig. 2, i.e. $\langle F(w)\rangle \simeq F_{\rm c}$. Since the effective trapping strength consists not only of the strength of the trap but also of the elastic modulus of the strands on which one pulls, it gets lowered while the molecule opens; for this reason we subtract the measured $\langle F(w)\rangle$ instead of its mean. Second, $\Delta(w,w')$ only depends on the difference $w-w'$. The resulting function is $\Delta(w-w')$. It also appears for the depinning of higher-dimensional elastic objects of dimension d, as e.g. a magnetic domain wall in a bulk magnet ($d=2$), or a contact line ($d=1$). Then $F(w)$ is the force acting on the center of mass. These systems are governed by an equation of motion for the domain wall or line u, parameterized by an internal d-dimensional coordinate x and time t,

$$\partial_t u(x,t) = \nabla^2 u(x,t) + m^2\left[w-u(x,t)\right] + F\big(x,u(x,t)\big)\,. \tag{3}$$

Then [25–27]

$$\Delta(w-w') := \frac{1}{L^d}\,\langle F(w)F(w')\rangle^{\rm c}\,, \tag{4}$$

where L is the linear size of the system, and L^d its volume. Despite the complexity of the problem, analytical methods have been devised to obtain $\Delta(w)$ from first principles [19, 20, 23, 27]. These methods are based on a field theory for the equation of motion (3). Field theory is a central tool in theoretical physics [28], with applications ranging from elementary particle physics [29] to the fluctuations observed around the critical point in liquid-gas transitions [30]. In all these cases, a set of *flow equations* for a finite number of *coupling constants* is derived. These methods fail for disordered systems as those given by Eq. (3). A way out was found by realizing that the flow for the coupling constants has to be generalized to flow equations for a function. This is known as the *functional renormalization group* (FRG). The flow-equations take the form

$$\partial_\ell \Delta(w) = -\frac{\mathrm{d}^2}{\mathrm{d}w^2}\frac{1}{2}\left[\Delta(w)-\Delta(0)\right]^2 + \ldots \tag{5}$$

where the omitted terms are higher-order corrections (technically higher-loop terms [22–24, 28]), equivalent to an expansion in $\varepsilon = 4-d$ (with d the dimension of the object). What came as a surprise was the realization that $\Delta(w)$ appearing in Eq. (5), when integrated from a microscopic scale to the length scale $\ell \equiv 1/m$ is the disorder-force correlator measured via Eq. (4) [25–27]. Measuring $\Delta(w)$ is thus a key test [13, 31, 32] for the field theory of disordered systems. The solution to Eq. (5) (leading order in the expansion parameter ε) reads

$$\Delta(w) = \mathcal{A}\,\Delta_{\rm FT}(w/\rho)\,, \tag{6}$$

$$\Delta_{\rm FT}(x) = -W\Big(-\exp\big(-\tfrac{x^2}{2}-1\big)\Big)\,, \tag{7}$$

where $\mathcal{A}$ and ρ are non-universal constants, and the product-log $W(z)$ is the principal solution for w in $z = we^w$. Field theory also applies to the experiment described above, which has (internal) dimension $d=0$ (the single degree of freedom is the number of the last unpeeled monomer). While the expansion parameter $\varepsilon = 4$ is rather large, we are in the fortunate position to have an alternative solution [33], namely for a particle dragged through a disordered force landscape as given by Eq. (3), dropping the non-existing index x there. What remains to be specified is the distribution of forces F. Since the

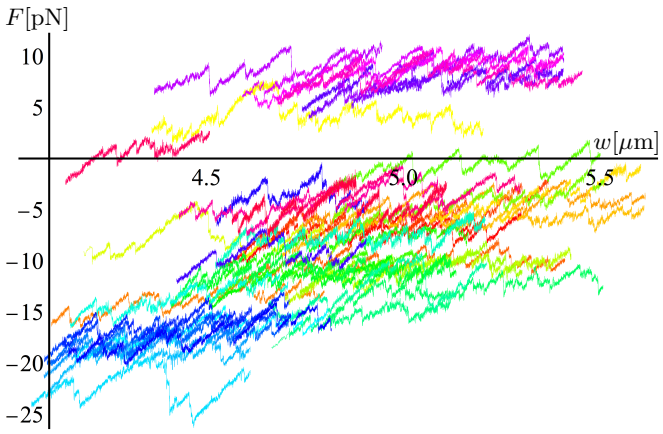

FIG. 3: Force-extension curves restricted to the plateau region for one of our batches with 47 data sets. Curves are randomly displaced for better visualization.

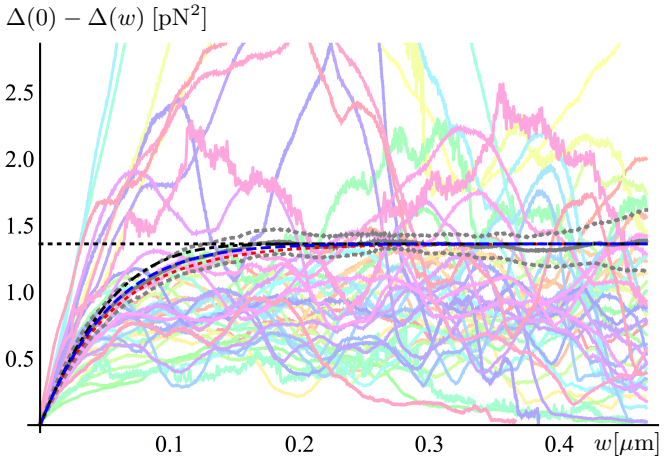

FIG. 4: Estimation of $\Delta(0)-\Delta(w)$ from one of our batches with 47 datasets, compared to three theoretical curves: pure exponential decay (red), 1-loop FRG (black dot-dashed), and toy model (blue dashed).

microscopic forces can be thought of as sums of random variables (neighboring monomers act together to generate these random forces), and assuming the central-limit theorem applies, forces are Gauss-distributed (with assumed variance 1), which in the terminology of [33] leads to the Gumbell universality class of extreme-value statistics, with correlator

$$\Delta(w) \;=\; m^4\rho_m^2\Delta_{\rm Gumbell}(w/\rho_m)\;, \tag{8}$$

$$\Delta_{\rm Gumbell}(x) := \frac{x^2}{2} + {\rm Li}_2\left(1-{\rm e}^{|x|}\right) + \frac{\pi^2}{6}\;, \tag{9}$$

$$\rho_m \;=\; \frac{1}{m^2\sqrt{2\ln(m^{-2})}}\;. \tag{10}$$

III. DATA-ANALYSIS

We measure the force-extension curve in an RNA-DNA-unzipping experiment [3–5], retaining from the force-extension curve shown on Fig. 2 only the plateau part (in red). This experiment was repeated 163 times. From one of the batches with 47 data sets, we show the retained plateaux on Fig. 3. In order to minimize statistical errors, we measure the combination $\Delta(0)-\Delta(w)=\frac{1}{2}\left\langle[F(u+w)-F(u)]^2\right\rangle^{\rm c}$. This average is more stable experimentally, since there seems to be a small drift in the data (visible on Fig. 3); the latter may be induced by a slightly diminishing effective stiffness m^2 while opening the strands, even though this effect is not visible on Fig. 2.

On figure 4, we show the combination $\Delta(0)-\Delta(w)$ as defined by Eq. (4), for each of the force-extension curves of Fig. 3, with the shaded colors identical to those of Fig. 3. Strong statistical fluctuations are visible. Their mean, in solid grey, is compared to three theoretical curves: The leading-order field theory result (7) (black dot-dashed line), the Gumbell result (8) (blue, dashed), and an exponentially decaying function (red, dotted). There are two unknown scales, equivalent to a rescaling of w and Δ. Since the slope at the origin can be measured precisely, we rescale all functions to have the same slope [39]. The remaining parameter is the behavior of $\Delta(0)-\Delta(w)$ for large w, which is adjusted visually. In dotted gray we show our estimates of the absolute error bars, obtained by resampling, as explained in appendix A.

The result (of these partial data) favors the theoretical prediction (8), while the estimated error bars are seemingly rather large. The reason for the latter is that the main statistical fluctuations come from the amplitude multiplying $\Delta(w)$. Indeed, rescaling this amplitude to one in each of our resampled samples, and measuring the remaining statistical error, results in a much smaller error estimate. This is presented on our final curve on Fig. 5, where we now give the function $\Delta(w)$ directly, using all our data. The errors are given by the green shaded region. The agreement of the theory and the experimental data is excellent, better than expected from the single measurements of Fig. 4. This strongly indicates that the *universal physics* behind the depinning transition is robust. One surprise to us was that thermal fluctuations, which are non-neglible, do not spoil the result, as theory even predicts a rounding of the cusp [27], a feature we clearly do not see. However thermal fluctuations are visible leading to an additional constant term for $\Delta(w)$ at $w=0$, but not for $w>0$, of amplitude $0.055{\rm pN}^2$, and which has been subtracted in Fig. 4. It would on Fig. 5 shift up the first point $\Delta(0)$. This thermal noise is seemingly noise of the beads hit by the water molecules, and not noise for the effective degree of freedom u in Eq. (3).

IV. INTERPRETATION AND CONCLUSION

Our final result for $\Delta(w)$, given by the grey solid line on Fig. 5, is in remarkable agreement with the analytical result (8). What does this mean? Consider again Fig. 2, where one notes that the force grows linearly, interrupted by sudden drops of size δF. One can show [34] that the derivative of the function $\Delta(w)$ at the origin is related to a moment ratio

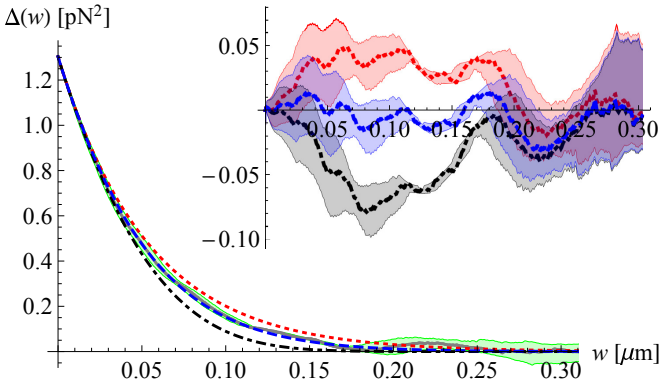

FIG. 5: Measurements of $\Delta(w)$ (in grey), with $1-\sigma$ error bars (green shaded), compared to three theoretical curves: pure exponential decay (dotted red), 1-loop FRG (black dot-dashed), and toy model (blue dashed). Inset: theoretical curves with the data subtracted (same color code). The blue curve is the closest to the data.

of force drops [40]

$$|\Delta'(0^+)| = m^2 \delta F_m \,, \qquad \delta F_m = \frac{\langle \delta F^2 \rangle}{2 \langle \delta F \rangle} \,. \tag{11}$$

Our experiments yield $m^2 = 55 \pm 5\,\mathrm{pN}/\mu\mathrm{m}$ (see Fig. 1) leading to $\delta F_m = 0.43 \pm 0.05\,\mathrm{pN}$, and to a correlation length $\xi = 0.055 \pm 0.005 \mu\mathrm{m} \simeq 186$ base pairs. This is roughly consistent with the 9 force drops identifiable on figure 2. The driving velocity was varied from 5 to 7 $\mathrm{nm/s}$, where no statistically significant difference could be observed for $\Delta(w)$.

These measurements indicate a serious challenge for unzipping experiments using optical tweezers: As force-force correlations decay on a scale of about 200 bases, which is about $1/15$ of the length of the ribosomal RNA, events can be resolved with a resolution of about 200 nucleotides. As Eq. (10) shows, this resolution is higher when the stiffness m^2 is higher. The key to a high resolution is thus a well-aligned trap: If the trap is not optimally aligned, showing the critical force at a say 20% smaller value, the resolution suffers according to Eqs. (8)-(10) by approximately the same amount. Another possibility to increase the stiffness is to use shorter constructions.

On the theoretical side, both formulas (7) and (8) are obtained at depinning, i.e. out-of-equilibrium, and not in thermal equilibrium, where the corresponding curves look rather different, with one zero-crossing and a vanishing integral [22, 24, 27, 35]. While the sequence used in the experiments is extracted from ribosomal RNA, thus is *not random*, the measured function $\Delta(w)$ agrees to a good precision with the result obtained for a *random* sequence. Also note that the chosen system maximises the force differences, and thus the measured signal $\Delta(w)$, as the two possible parings CG and AT/AU have different binding energies, and appear almost in the same proportion [3].

A surprising feature is that while *thermal fluctuations* are clearly visible in the experiment, they do not lead to a *rounding of the cusp*, contrary to expectations in the literature [27, 36]. The measured $\Delta(w)$ can be compared to the same signal measured for the depinning of a contact line [13], or numerical simulations for magnetic domain walls at equilibrium [31] or a string at depinning [32]. The latter are well approximated by the field-theoretical result, obtained in an expansion in $d = 4 - \varepsilon$. This expansion works best for d close to $d = 4$, but can be extrapolated down to $d = 1$ [32], using the field theory results of [22, 23], and in principle down to $d = 0$, the case considered here [41]. Using the exact result of Eq. (8) avoids errors due to the expansion. Comparing these studies with our experiment, a clear dependence on the dimension is observed.

[1] Z.D. Stephens, S.Y. Lee, F. Faghri, R.H. Campbell, C. Zhai, M.J. Efron, R. Iyer, M.C. Schatz, S. Sinha and G.E. Robinson, *Big data: Astronomical or genomical?*, PLOS Biology **13** (2015) 1–11.

[2] A. Ashkin, *Acceleration and trapping of particles by radiation pressure*, Phys. Rev. Lett. **24** (1970) 156–159.

[3] M. Bercy, *Structures secondaires dans l'ARN: une étude par mesure de forces sur molécules uniques*, PhD thesis, PSL Research University, 2015.

[4] L. Melkonyan, *Early stages of ribosome assembly, studied by single-molecule force measurements*, PhD thesis, PSL Research University, 2018.

[5] L. Melkonyan, M. Bercy, T. Bizebard and U. Bockelmann, *Overstretching double-stranded RNA, double-stranded DNA, and RNA-DNA duplexes*, Biophysical Journal **doi: 10.1016/j.bpj.2019.07.003** (2019).

[6] S.L. Gotta, O.L. Miller and S.L. French, *rRNA transcription rate in escherichia coli*, J. Bacteriol. **173** (1991) 6647–6649.

[7] J.F. Léger, G. Romano, A. Sarkar, J. Robert, L. Bourdieu, D. Chatenay and J.F. Marko, *Structural transitions of a twisted and stretched dna molecule*, Phys. Rev. Lett. **83** (1999) 1066–1069.

[8] T.R. Strick, J.-F. Allemand, D. Bensimon, A. Bensimon and V. Croquette, *The elasticity of a single supercoiled dna molecule*, Science **271** (1996) 1835–1837.

[9] I. De Vlaminck and C. Dekker, *Recent advances in magnetic tweezers*, Ann. Rev. Biophys. **41** (2012) 453–472.

[10] D.R. Nelson, *Statistical physics of unzipping DNA*, in A. T. Skjeltorp and A. V. Belushkin, editors, *Forces, Growth and Form in Soft Condensed Matter: At the Interface between Physics and Biology*, pages 65–92, Springer Netherlands, Dordrecht, 2005.

[11] H. Barkhausen, *Zwei mit Hilfe der neuen Verstärker entdeckte Erscheinungen*, Phys. Z. **20** (1919) 401–403.

[12] J.P. Sethna, K.A. Dahmen and C.R. Myers, *Crackling noise*, Nature **410** (2001) 242–250.

[13] P. Le Doussal, K.J. Wiese, S. Moulinet and E. Rolley, *Height fluctuations of a contact line: A direct measurement of the renormalized disorder correlator*, EPL **87** (2009) 56001, arXiv:0904.4156.

[14] B. Gutenberg and C. F. Richter, *Earthquake magnitude, intensity, energy, and acceleration*, B. Seismol. Soc. Am. **46** (1956) 105–145.

[15] G. Blatter, M.V. Feigel'man, V.B. Geshkenbein, A.I. Larkin and V.M. Vinokur, *Vortices in high-temperature superconductors*, Rev. Mod. Phys. **66** (1994) 1125.

[16] R. Burridge and L. Knopoff, *Model and theoretical seismicity*, B. Seismol. Soc. Am. **57** (1967) 341–371.

[17] B. Alessandro, C. Beatrice, G. Bertotti and A. Montorsi, *Domain-wall dynamics and Barkhausen effect in metallic ferromagnetic materials. I. Theory*, J. Appl. Phys. **68** (1990) 2901.

[18] B. Alessandro, C. Beatrice, G. Bertotti and A. Montorsi, *Domain-wall dynamics and Barkhausen effect in metallic ferromagnetic materials. II. Experiments*, J. Appl. Phys. **68** (1990) 2908.

[19] T. Nattermann, S. Stepanow, L.-H. Tang and H. Leschhorn, *Dynamics of interface depinning in a disordered medium*, J. Phys. II (France) **2** (1992) 1483–8.

[20] O. Narayan and D.S. Fisher, *Threshold critical dynamics of driven interfaces in random media*, Phys. Rev. B **48** (1993) 7030–42.

[21] H. Bucheli, O.S. Wagner, V.B. Geshkenbein, A.I. Larkin and G. Blatter, *$(4+N)$-dimensional elastic manifolds in random media: a renormalization-group analysis*, Phys. Rev. B **57** (1998) 7642–52.

[22] P. Chauve, P. Le Doussal and K.J. Wiese, *Renormalization of pinned elastic systems: How does it work beyond one loop?*, Phys. Rev. Lett. **86** (2001) 1785–1788, cond-mat/0006056.

[23] P. Le Doussal, K.J. Wiese and P. Chauve, *2-loop functional renormalization group analysis of the depinning transition*, Phys. Rev. B **66** (2002) 174201, cond-mat/0205108.

[24] P. Le Doussal, K.J. Wiese and P. Chauve, *Functional renormalization group and the field theory of disordered elastic systems*, Phys. Rev. E **69** (2004) 026112, cond-mat/0304614.

[25] P. Le Doussal, *Finite temperature Functional RG, droplets and decaying Burgers turbulence*, Europhys. Lett. **76** (2006) 457–463, cond-mat/0605490.

[26] P. Le Doussal and K.J. Wiese, *How to measure Functional RG fixed-point functions for dynamics and at depinning*, EPL **77** (2007) 66001, cond-mat/0610525.

[27] K.J. Wiese and P. Le Doussal, *Functional renormalization for disordered systems: Basic recipes and gourmet dishes*, Markov Processes Relat. Fields **13** (2007) 777–818, cond-mat/0611346.

[28] J. Zinn-Justin, *Quantum Field Theory and Critical Phenomena*, Oxford University Press, Oxford, 1989.

[29] Steven Weinberg, *The Quantum Theory of Fields*, Volume *1-3*, Cambridge University Press, 1995.

[30] C. Domb, M.S. Green and J. Lebowitz, editors, *Phase Transitions and Critical Phenomena*, Volume *1-19*, Academic Press, London, 1972-2001.

[31] A.A. Middleton, P. Le Doussal and K.J. Wiese, *Measuring functional renormalization group fixed-point functions for pinned manifolds*, Phys. Rev. Lett. **98** (2007) 155701, cond-mat/0606160.

[32] A. Rosso, P. Le Doussal and K.J. Wiese, *Numerical calculation of the functional renormalization group fixed-point functions at the depinning transition*, Phys. Rev. B **75** (2007) 220201, cond-mat/0610821.

[33] P. Le Doussal and K.J. Wiese, *Driven particle in a random landscape: disorder correlator, avalanche distribution and extreme value statistics of records*, Phys. Rev. E **79** (2009) 051105, arXiv:0808.3217.

[34] P. Le Doussal and K.J. Wiese, *Size distributions of shocks and static avalanches from the functional renormalization group*, Phys. Rev. E **79** (2009) 051106, arXiv:0812.1893.

[35] C. Husemann and K.J. Wiese, *Field theory of disordered elastic interfaces to 3-loop order: Results*, Nucl. Phys. B **932** (2018) 589–618, arXiv:1707.09802.

[36] P. Chauve, T. Giamarchi and P. Le Doussal, *Creep and depinning in disordered media*, Phys. Rev. B **62** (2000) 6241–67, cond-mat/0002299.

[37] We show below that the signal specified in Eq. (4) is the same as that obtained by supposing a random force.

[38] The stiffness per trap is about $250\mathrm{pN}/\mu\mathrm{m}$ [3], leading to half this value for the two traps. At the plateau start, the strands reduce this to $m^2 = 55 \pm 5\mathrm{pN}/\mu\mathrm{m}$, see Fig. 1.

[39] For the noisy data at hand, this procedure is more stable than the one used in Refs. [13, 31, 32], where $\Delta(w)$ was rescaled to have integral 1.

[40] In Ref. [34] drops in position u of size S are considered, related via Eq. (1) to force drops as $\delta F = m^2 S$.

[41] A Padé approximant of the form $\Delta(u) = \Delta_1(u) g_\beta(\Delta_2(u)/\Delta_1(u))$ with $g_\beta(x) = (1+\beta x)/(1+(\beta-1)x)$ and $\beta = 1/2$ gives a quite good approximation to Eq. (8), whereas a direct extrapolation ($\beta = 1$) does not.

Appendices – Supplementary Material

Appendix A: Data analysis and error-estimates

Protocal and error-estimates: Define for a data-set $\mathcal{D}_i$, with $i = 1, ..., n$ and n the total number of force-extension curves, the set-average

$$N_i(w) := \sum_{u\in\mathcal{D}_i} \tag{A1}$$

$$Q_i(w) := \frac{1}{N_i(w)} \sum_{u\in\mathcal{D}_i} \Big[F(u+w) - F(u)\Big]^2 \tag{A2}$$

$$M_i(w) := \frac{1}{N_i(w)} \sum_{u\in\mathcal{D}_i} \Big[F(u+w) - F(u)\Big] \tag{A3}$$

$$Q_i^{\rm c}(w) := Q_i(w) - M_i(w)^2 \tag{A4}$$

The above sums run over all values u, for which exists a pair $F(u+w)$ and $F(u)$; $N_i(w)$ is the number of such pairs. Our best estimate for the force-force correlator then is

$$\Big\langle \Big[F(u+w) - F(u)\Big]^2 \Big\rangle^{\rm c} = \frac{\sum_i Q_i^{\rm c}(w) N_i(w)}{\sum_i N_i(w)} \,. \tag{A5}$$

The fluctuations of the data shown on Fig. 4 are very large, making error-estimates difficult. We used a statistical resampling technique: Randomly divide all datasets $\mathcal{D}_i$ into two parts, $\mathcal{P}_1$ and $\mathcal{P}_2$. Define

$$N_{\mathcal{P}_1}(w) := \sum_{i\in\mathcal{P}_1} N_i(w) \,, \tag{A6}$$

$$Q^{\rm c}_{\mathcal{P}_1}(w) := \frac{1}{N_{\mathcal{P}_1}(w)} \sum_{i\in\mathcal{P}_1} Q_i^{\rm c}(w) N_i(w) \,. \tag{A7}$$

A similar definition holds for $\mathcal{P}_2$. Then for each w measure the variance of the partial means $Q^{\rm c}_{\mathcal{P}_1}(w)$ and $Q^{\rm c}_{\mathcal{P}_2}(w)$. Finally, average over all partitions $\Pi_i, \{1, ..., n\} \to \mathcal{P}_1, \mathcal{P}_2$. In practice, it is enough to take $N_{\rm p} = 100$ random partitions. The error estimate then is

$$\sigma^2(w) := \frac{1}{N_{\rm p}} \sum_{\Pi_i} \left\langle \frac{1}{2} \sum_{k=1}^{2} \Big[Q^{\rm c}_{\mathcal{P}_k(\Pi_i)}(w) - Q^{\rm c}(w)\Big]^2 \right\rangle \tag{A8}$$

$$N_{\rm p} := \sum_{\Pi_i} \tag{A9}$$

We can also define the set of all $2N_{\rm p}$ partial means,

$$\mathcal{A}(w) := \bigcup_{\Pi_i} \bigcup_{k=1,2} Q^{\rm c}_{\mathcal{P}_k(\Pi_i)}(w) \,. \tag{A10}$$

We find that our analysis is consistent, with

$$\mathrm{var}\Big(\mathcal{A}(w)\Big) \approx \sigma^2(w) \,. \tag{A11}$$

These error estimates are absolute errors, presented on Fig. 4. To obtain the error estimate given on Fig. 5, the partial means (A10) where rescaled such that their w-integrals equal the w-integral over all samples. This takes out amplitude fluctuations, reducing the errors to errors of the shape.

Appendix B: Check on test data

We generated test data according to the following protocol: For each real data set, sample an Ornstein-Uhlenbeck process of the same length, with mean $F_m = F_c$, variance $\Delta(0)$, and correlation length ξ as measured. This is achieved by the stochastic process

$$F(w+\delta w) = F(w) + \zeta(w)\sqrt{\frac{\Delta(0)}{\xi}} + \frac{F_m - F(w)}{\xi} \,, \tag{B1}$$

$$\langle \zeta(w)\zeta(w')\rangle = \delta_{w,w'} \,. \tag{B2}$$

This gives a first set of test data. For a second set, we add an additional white noise in the x-direction, with $\delta x \in \{-1, 0, 1\}$, in units of the resolution of the measuring mashine. For a third set, we added a Gauss-distribution of mean zero and width 1 to the force signal. By construction, these test-data are exponentially correlated

$$\langle F(w)F(w')\rangle^{\rm c} = \Delta(0)\mathrm{e}^{-|w-w'|/\xi} \,, \tag{B3}$$

with additional noise for sets 2 and 3. They should thus approach the red dotted curve of Fig. 5. This is indeed observed, with an appropriate estimate for the error bars.